RNA (2002), *8*:816–823. Cambridge University Press. Printed in the USA.

DOI: 10.1017.S1355838202026730

Probing FinO–FinP RNA interactions by site-directed protein–RNA crosslinking and gelFRET

ALEXANDRU F. GHETU,[1] DAVID C. ARTHUR,[1] TOM K. KERPPOLA,[2] and J.N. MARK GLOVER[1]

[1]Department of Biochemistry, University of Alberta, Edmonton, Alberta, T6G 2H7, Canada
[2]Howard Hughes Medical Institute and Department of Biological Chemistry, University of Michigan Medical School, Ann Arbor, Michigan 48109-0650, USA

ABSTRACT

The conjugative transfer of F-plasmids is repressed by a two-component system, which consists of the antisense RNA FinP and the protein FinO. FinO binds FinP, protecting it from endonucleolytic degradation and facilitating duplex formation between FinP and its complementary RNA. Here we present the results of site-specific protein–RNA crosslinking and gel-based fluorescence resonance energy transfer (gelFRET) experiments used to probe the structure of a complex of FinO bound to an RNA target consisting of a duplex with 5′ and 3′ single-stranded tails. The crosslinking experiments reveal that an extensive, largely positively charged surface on FinO contacts RNA. The gelFRET measurements indicate that the 5′ single-stranded tail of the RNA is in closer contact with much of the protein than the distal, blunt end of the RNA duplex. These data suggest that significant conformational adjustments in the protein and/or the RNA accompany complex formation.

Keywords: conjugation; protein–RNA interactions; site-specific crosslinking

INTRODUCTION

Plasmid conjugation is a major mechanism for transfer of antibiotic resistance and virulence determinants between bacteria (Mazodier & Davies, 1991). Perhaps the best studied group of conjugative plasmids is the F family. F plasmids contain a large, multicistronic transfer (*tra*) operon, which encodes the majority of proteins required for conjugation (Frost et al., 1994). Transcription of the *tra* operon is positively regulated by the plasmid-encoded product of the *traJ* gene (Mullineaux & Willetts, 1985). The production of TraJ is, itself, negatively regulated by a two-component repression system consisting of FinP, an RNA that is antisense to the 5′ end of *traJ* mRNA, and FinO, a 21.5-kDa RNA binding protein (Finnegan & Willetts, 1972). Duplex formation between FinP and *traJ* mRNA occludes the ribosomal binding site and prevents translation of *traJ* RNA (van Biesen & Frost, 1994). An RNase E recognition site located between the two stem-loops of FinP makes this RNA highly susceptible to degradation (Jerome et al., 1999). FinO binds to both FinP and *traJ* mRNA, protecting FinP from degradation and enhancing the rate of duplex formation between FinP and *traJ* mRNA (Lee et al., 1992; van Biesen et al., 1993; Koraimann et al., 1996; Jerome et al., 1999; Ghetu et al., 2000).

Recent results have begun to reveal the molecular mechanism underlying FinOP function. Biochemical studies have shown that FinO binds as a monomer to stem-loop structures with short 5′ and 3′ single-stranded tails (Ghetu et al., 1999; Jerome & Frost, 1999; Fig. 1A). These interactions are not sequence specific, so that complementary stem-loops with single-stranded tails, such as stem-loop II (SLII) of FinP and the complementary stem-loop in *traJ* RNA are bound with nearly identical affinities (Jerome & Frost, 1999). The crystal structure of FinO revealed an elongated, largely helical structure reminiscent of a right-handed fist with an extended index finger and a thumb, touching the index finger near its base (Fig. 2). The finger corresponds to a solvent-exposed N-terminal helix (α1), and the thumb corresponds to the C-terminal-most helix (α6). An extended, positively charged surface composed of parts of α1, α6 and the fist was suggested to contact RNA targets (Ghetu et al., 2000). The N-terminal 25 residues

Reprint requests to: J.N. Mark Glover, Department of Biochemistry, University of Alberta, Edmonton, Alberta, T6G 2H7, Canada; e-mail: mark.glover@ualberta.ca.

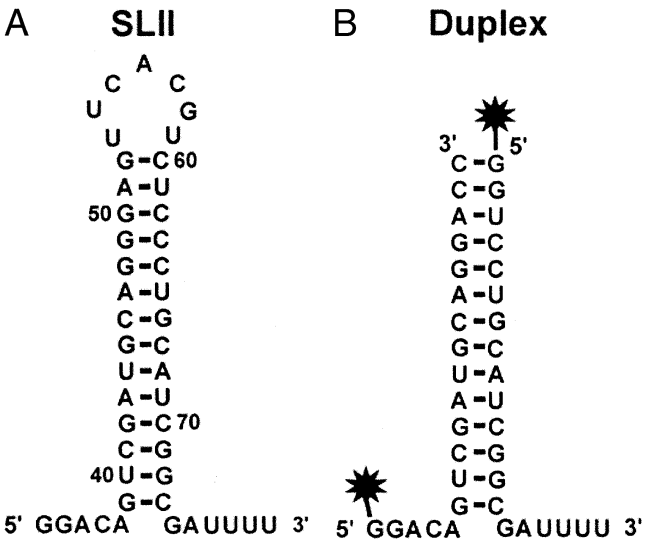

FIGURE 1. Schematic representation of SLII-based RNAs used in this study. **A:** The nucleotide sequence and predicted secondary structure of SLII. **B:** The nucleotide sequence and secondary structure of the RNA duplex used in our experiments. Sites where fluorescein has been attached to the duplex are indicated. The duplex differs from SLII in that the loop is absent and the first three base pairs at the top of the stem are reordered.

of FinO are not present in the crystal structure and are not required for binding to individual RNA substrates; however, the N-terminus facilitates sense–antisense RNA interactions between FinP and *traJ* RNAs (Ghetu et al., 2000). We have suggested (Ghetu et al., 2000) that the N-terminus of FinO may directly interact with an initial "kissing complex" formed between complementary loops in FinP and *traJ* RNAs (Koraimann et al., 1991), thereby facilitating FinP-*traJ* RNA recognition. This possibility, together with the structure of FinO, provided the basis for a model of FinO bound to SLII from FinP (Ghetu et al., 2000). In this model, the stem-loop of SLII lies along the exposed, positively charged α1 of FinO so that the N-terminus is positioned near the SLII loop to participate in loop-loop recognition. The single-stranded tails at the base of the stem interact with a large positively charged patch on the globular body of the protein.

We have used site-specific protein–RNA crosslinking and a gel-based fluorescence resonance energy transfer (gelFRET) assay to investigate the interactions between FinO and SLII. The results of the crosslinking experiments reveal an extensive surface on FinO that comes into contact with RNA. The gelFRET experiments allowed us to map the relative proximity of specific sites on FinO and FinP and indicated that the single-stranded tails at the base of the duplex are in much closer proximity to FinO than is the opposite end of the duplex proximal to the loop. These data suggest that FinO binding to SLII RNA may involve conformational changes in FinO, SLII, or both.

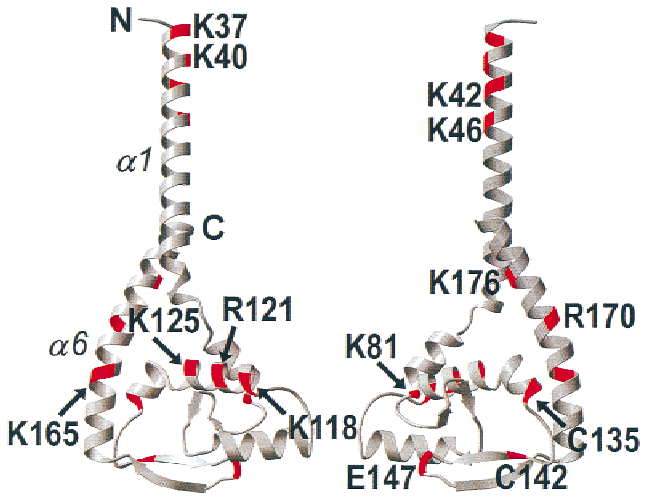

FIGURE 2. The structure of FinO and the positions of single cysteine substitutions. Two ribbons diagrams of FinO, related by a 180° rotation about a vertical axis. The positions of cysteine substitutions that serve as sites of attachment for APA or Texas Red are indicated in red. Also indicated in the figure are the N- and C-terminal ends of FinO and α-helices 1 and 6.

RESULTS AND DISCUSSION

Site-specific FinO-SLII RNA crosslinking

To experimentally determine the regions of FinO that are in close proximity to the target RNA, we used a site-specific crosslinking assay involving the photoactivated crosslinker, azidophenacyl bromide (APA-Br). We first replaced the three native cysteine residues in FinO with serines and used a gel electrophoretic mobility shift assay to show that these three substitutions do not alter the affinity of FinO binding to the RNA (data not shown). We next created a set of FinO mutants that contain single cysteine substitutions at various solvent-exposed positions, to which we could attach APA via a thioester linkage (Fig. 2). The sites of substitution include the positively charged surfaces on the tip of the N-terminal helix, the body of the protein, the C-terminal helix and the negatively charged surface on the bottom of the molecule.

APA-modified FinO mutants were incubated either with SLII RNA, a minimal RNA target for FinO (Jerome & Frost, 1999) or tRNA, which does not bind FinO with high affinity (van Biesen & Frost, 1994; Sandercock & Frost, 1998; Ghetu et al., 1999). Crosslinking was induced by irradiation of the APA-modified protein/RNA complexes with UV light, which activates the azido functional group of APA. The resulting nitrene reacts in a nonspecific manner with protein or RNA that is within an ~10 Å radius of the modified cysteine (Pendergrast et al., 1992; Chen & Ebright, 1993). The reaction products were separated by a denaturing polyacrylamide

gel and the gel was stained with Coomassie blue and ethidium bromide to visualize protein and RNA, respectively (Fig. 3A). FinO-SLII crosslinking was detected by the presence of high molecular weight species that contain both protein and RNA. As a negative control, the APA-treated cysteine-free FinO mutant protein does not crosslink to SLII under these conditions. The specificity of the FinO-SLII crosslinking was demonstrated by the finding that tRNA is not efficiently crosslinked by the same APA-modified FinO samples in parallel experiments carried out under identical solution conditions and protein/RNA concentrations.

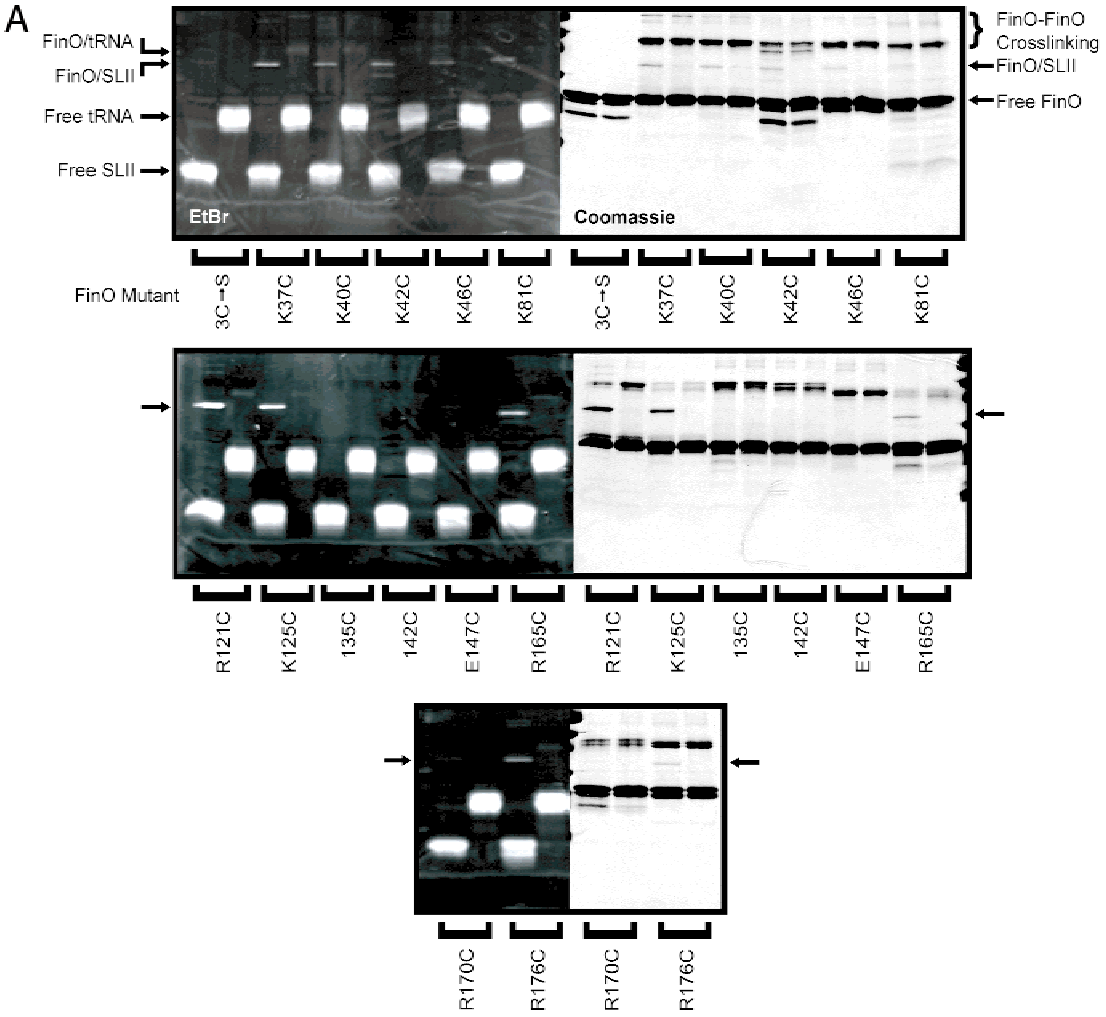

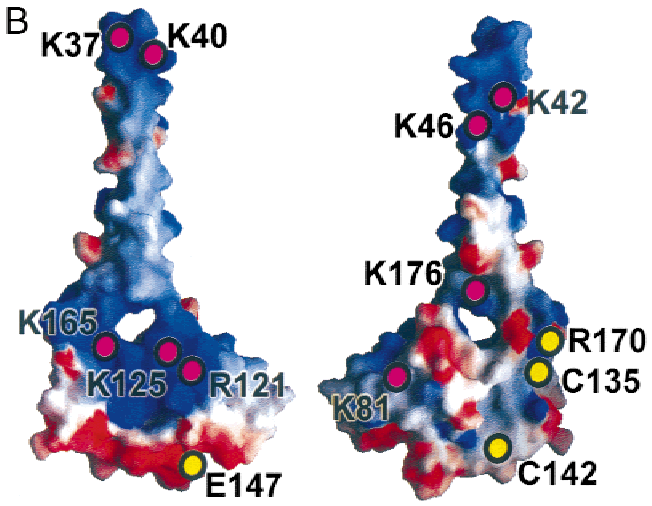

FIGURE 3. Site specific crosslinking of FinO and SLII. **A:** Crosslinked protein/RNA complexes were analyzed by SDS-PAGE in which RNA-containing species were visualized by ethidium bromide staining (left), and protein-containing species were detected by Coomassie blue staining (right). Indicated on the bottom of each gel pair are the various FinO cysteine mutants used. Indicated to the left of the top ethidium bromide stained gel are the positions of free SLII, free tRNA, the FinO/SLII crosslinked product containing one protein bound to one SLII (resulting from specific interactions), and the FinO/tRNA crosslinked product (resulting from nonspecific interactions). To the right of the top Coomassie stained gel are the positions of free FinO, the FinO/SLII crosslinked product, and nonspecific crosslinking products between FinO molecules. Indicated by arrows on the bottom two gel pairs is the position of the FinO/SLII crosslinked product. C → S indicates a protein in which all the native cysteine residues have been replaced with serine. **B:** Two electrostatic surface representations of FinO, in the same orientations as shown in Figure 2A. Magenta circles indicate the sites of APA attachment that showed significant crosslinking to SLII RNA, and yellow circles indicate sites that do not crosslink to RNA.

Significant levels of crosslinking to SLII RNA, but not to tRNA, were observed for many of the APA-modified residues within positively regions of the FinO surface (Fig. 3A). The most efficient crosslinking was observed for residues 121 and 125, which are exposed on the surface of α4, as well as residue 165, which together constitute part of the large positively charged surface on the main body of the protein (Fig. 3B). Weaker but significant levels of crosslinking were also observed between modified residues at the positively charged tip of the N-terminal FinO helix (residues 37, 40, 42, and 46), as well as residue 176 near the C-terminus of α6. These results confirm that these two positively charged regions are in close proximity to the RNA substrate and likely play a significant role in recognizing specific target stem-loop structures. Weak crosslinking was also observed between APA-modified residue 81 and SLII RNA. Residue 81 is on the body of FinO, but on the opposite face from the major positively charged surface. As predicted (Ghetu et al., 2000), crosslinking was not observed when APA was positioned on the negatively charged region of FinO (residues 142 and 147), nor were appreciable levels of RNA crosslinking observed for APA-modified residues 135 or 170, suggesting that these regions are not in direct contact with RNA. These results are summarized in Figure 3B and indicate that the N-terminal helix and the positively charged surface on the body of the protein are in closest contact with RNA. However, interactions also occur on the opposite face of the protein, possibly due to the wrapping of the SLII tails around FinO.

Probing FinO-RNA architecture using gelFRET

We have previously suggested that FinO and SLII RNA interact such that the long axis of FinO is parallel to the stem, the positively charged surface on the core of FinO is in contact with the base of the stem, and the N-terminus of α1 lies near the SLII loop. To test this model, we used a gelFRET analysis in which the RNA is labeled with the donor fluorophore fluorescein and the protein is labeled at single, specific sites with the receptor fluorophore Texas Red. The fluorescent complexes are separated by nondenaturing gel electrophoresis and the FRET from the individual complexes is analyzed by excitation of the separated complexes within the gel. In this way, fluorescence from unbound protein, RNA, and nonspecific protein–RNA complexes can be eliminated and the relative efficiencies of energy transfer between donor and acceptor molecules at different positions on the protein and nucleic acid components can be assessed (Ramirez-Carrozzi & Kerppola, 2001a). This method has been used to determine the orientation of Fos-Jun heterodimer binding at different AP-1 binding sites (Diebold et al., 1998; Leonard & Kerppola, 1998; Ramirez-Carrozzi & Kerppola, 2001b, 2001c, 2001d). Here we present the first use of gelFRET to study protein–RNA complexes.

For our experiments, we have prepared two different RNA duplexes that are labeled on their 5′ ends with the donor fluorophore fluorescein. The 5′ ends of the two strands are located at opposite ends of the duplex RNA (Fig. 1B). These RNAs are based on SLII, but lack the single-stranded loop that connects the two strands in SLII. Using native gel electrophoresis, we determined dissociation constants of 4.8 ± 0.3 nM and 4.1 ± 0.5 nM for FinO binding to SLII and the RNA duplex, respectively. These results ensure that FinO binds the duplex substrate in a similar fashion to SLII and confirm previous results that the loop has no significant effect on the interaction between FinO and SLII RNA (Jerome & Frost, 1999). Our binding affinities are $\sim$20 times tighter than those determined previously (Jerome & Frost, 1999). These differences probably reflect changes in the gel mobility shift assay and improvements in the purification and quantitation of FinO.

FinO mutants labeled with Texas Red were mixed with an equi-molar amount of RNA labeled with fluorescein. The nucleoprotein complexes were separated from unbound FinO, unbound duplex, and free Texas Red by gel electrophoresis. The gel was scanned using a 488-nm argon-ion laser that excites fluorescein. The fluorescence emissions of both the donor fluorescein and acceptor Texas Red were measured at each position in the gel in separate scans. In Figure 4, the fluorescein and Texas Red fluorescent scans are overlaid so that the relative levels of fluorescein and Texas Red fluorescence in the different species in each lane can be qualitatively assessed. In these scans, green band color indicates fluorescein fluorescence, red color indicates Texas Red fluorescence, and yellow color indicates a mix of both fluorescein and Texas Red fluorescence. Thus, the degree of redness in bands corresponding to protein–RNA species gives a qualitative indication of the efficiency of energy transfer between the two fluorophores within that complex relative to the other complexes analyzed in parallel.

Labeling of FinO by the Texas Red fluorophore slightly altered the gel electrophoretic mobility for most of the FinO-RNA complexes (compare the mobilities of complexes labeled with Texas Red (+) to unlabeled complexes (−) in Fig. 4B). In cases where the complexes with and without acceptor could be separated, it was possible to ascertain that the analysis of the nucleoprotein complexes would not be influenced by the presence of unlabeled protein. The percentage of protein modified with Texas Red depended on the location of the cysteine residue, but was calculated to be greater than 60% in all cases examined (see Materials and Methods). In complexes labeled at residues 142 and 147, the Texas Red modification results in a more significant ($\sim$10%) reduction in the electrophoretic mobility of the complex. This may suggest that Texas Red

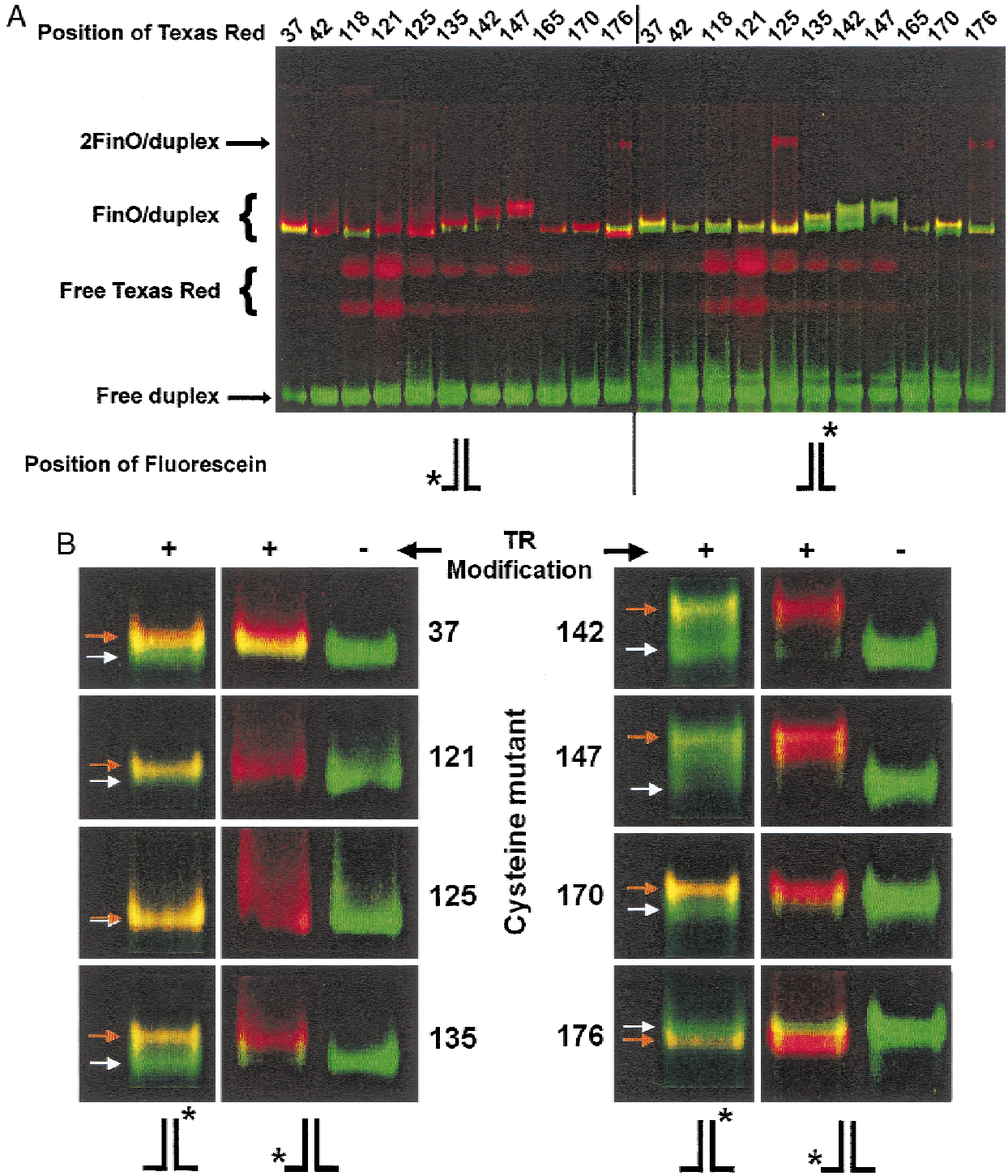

FIGURE 4. gelFRET analysis of the architecture of the FinO–RNA complex. Samples containing various Texas red-labeled FinO molecules and duplex RNA substrates labeled with fluorescein were separated by native gel electrophoresis. Fluorescence of the electrophoretically resolved species was excited directly in the gel. In the bands corresponding to the FinO-SLII complex, the color reflects the efficiency of energy transfer, with a red color indicating higher energy transfer, and therefore closer interfluorophore distance, than a green color. **A:** gelFRET analysis for Texas Red-labeled cysteine mutants bound to RNA duplex labeled with fluorescein either on the 5′ tail (left lanes) or the top of the duplex stem (right lanes). Indicated on the left of the figure are the positions of the free SLII RNA, FinO-SLII duplex, nonspecific complexes, and unincorporated Texas Red. The cysteine substitutions used are indicated above the lanes. **B:** Labeling of FinO with Texas Red leads to changes in the mobilities of several of the FinO-SLII complexes. Shown in this panel are the band shifts of Texas Red modified (lanes 1 and 2) or unmodified (lane 3) proteins in complex with duplex, labeled with fluorescein either on the 5′ tail (lane 1) or at the top of the stem (lanes 2 and 3). Each row represents a different cysteine point mutant, as indicated in the middle of the figure. Orange arrows indicate complexes with modified protein, and white arrows indicate complexes with unmodified proteins. Changes in mobility varied from one mutant to another. Although the addition of TR leads to changes in the mobility of most mutants, this was not the case for K125C.

modification at these residues alters the structure of FinO or the way in which the modified proteins interact with RNA.

Strikingly, energy transfer between the RNA and each of the labeled FinO proteins was higher when the fluorescein was positioned on the 5′ single-stranded tail of the RNA (left most lanes, Fig. 4A) compared to the opposite end of the duplex stem, where the loop would be found in SLII (right most lanes, Fig. 4A). This dramatic difference may suggest that all positions sampled on the surface of FinO are in closer proximity to the 5′ single-stranded tail of the RNA than the distal end of the duplex stem. Alternatively, these results could be explained by an inability of fluorescein to transfer energy to Texas Red when positioned at the blunt end of the duplex. This latter possibility is highly unlikely, however, due to the fact that nonspecific FinO-RNA complexes that are blunt-end-labeled with fluorescein show efficient energy transfer, whereas the specific complexes in the same lanes do not (compare colors of the low mobility, nonspecific, 2:1 FinO-RNA species with those of the specific complexes for the proteins labeled at residues 125 and 176 in Fig. 4A).

We previously suggested that the tip of the N-terminal helix of FinO contacts the RNA in or near the loop of SLII. However, our gelFRET results indicate that this part of the N-terminal α helix is, instead, much closer to the 5′ single-stranded tail. Moreover, our results indicate that not only are residues near the tip of α1 in close proximity to the 5′ tail, but residues within the main body of the protein are also close to the same region of the RNA. In the structure of the free protein, these residues are separated by as much as 65 Å, and it is therefore difficult to imagine a way that this pattern of energy transfer could occur without some reorganization of the protein structure upon RNA binding. It is possible that the solvent-exposed N-terminal helix of FinO might rearrange to allow its positively charged N-terminus to come into closer proximity with the main body of the protein, when bound to RNA. Indeed, the N-terminal helix is more flexible than the globular core of the protein, as shown by its susceptibility to limited proteolysis (Ghetu et al., 1999) and its overall high crystallographic B factor, relative to the rest of the structure (Ghetu et al., 2000).

The gelFRET results indicate that FinO binds to the single-stranded regions of the RNA target. However, single-stranded RNAs alone [such as the individual strands used in the gelFRET studies (data not shown) or RNA homopolymers (Jerome & Frost, 1999)] are not bound by FinO with high affinity, and therefore it seems likely that the region of the duplex proximal to the single-stranded tails is also contacted by FinO. The distal, blunt end of the RNA duplex is, in contrast, not contacted by the protein in a specific complex.

Interestingly, we have recently discovered that FinO can also alter the structure of its bound RNA substrate, destabilizing the duplex region in a process that ultimately contributes to sense–antisense RNA recognition and the repression of conjugation (A.F. Ghetu, D.C. Arthur, M.J. Gubbins, R.A. Edwards, L.S. Frost, & J.N. Mark Glover, submitted). Because the observed energy transfer is a weighted average of the energy transfer of the individual conformational states present during the measurement, such dynamic conformational changes in RNA structure could also have complex and profound effects on the observed energy transfer. For example, FinO might make intimate contact with the end of the duplex closest to the unpaired loop, but if the lifetime of this conformational state is short, it will not make a significant contribution to the observed FRET signal. Although we hope to probe the static structure of FinO-RNA complexes by X-ray crystallography, it seems likely that an understanding of the dynamic processes that may be critical to FinO function may require other, solution-based approaches, such as quantitative gelFRET experiments and NMR.

MATERIALS AND METHODS

Production of FinO cysteine point mutants

FinO and variants containing single cysteines were expressed as GST fusions from the pGEX-KG vector (Ghetu et al., 1999, 2000). All substitutions in FinO were introduced using the PCR overlapping amplification protocol (Ho et al., 1989). Initially, we constructed a cysteine-free *finO* clone, in which the codons encoding the three cysteines in the wild-type protein were mutated to serines. Cysteine codons were then substituted for the codons for residues Lys 37, Lys 40, Lys 42, Lys 46, Lys 81, Lys 118, Arg 121, Lys 125, Glu 147, Arg 165, Arg 170, or Lys 176. Proteins containing native cysteine residues at either position 135 or 142 were also prepared. DNA sequencing was used to confirm the presence of the cysteine substitutions. Expression and purification of all the cysteine mutants was as described (Ghetu et al., 1999). Protein concentrations were determined using the BIORAD Bradford assay, which was calibrated for true molar concentration by amino acid analysis. We used a dithionitrobenzoate assay (DTNB; Sigma; Hall & Fox, 1999) to determine the reactivity of the cysteine residues at pH 7.0. This assay revealed that at least 90% of the thiol groups were accessible to DTNB for each cysteine mutant.

Protein–RNA crosslinking

The RNA used in the crosslinking experiments, SLII, was produced by in vitro runoff transcription as described previously (Ghetu et al., 1999).

The crosslinker APA (Sigma) was initially dissolved in methanol to a final concentration of 208 mM. To attach APA to the cysteine mutants, 1 μL of the APA stock was added to 100 μL of an 80 μM protein solution containing the buffer 10 mM Tris, pH 7.0, 600 mM NaCl, and 1 mM EDTA. The reaction mixture was then incubated in the dark for 2 h at room temperature. Excess APA was subsequently removed using a BIORAD

P-30 spin column preequilibrated with 10 mM Tris, pH 7.0, 600 mM NaCl, and 1 mM EDTA.

The crosslinking reactions were performed with 42 μM protein and 81 μM SLII or yeast tRNA (Type X, Sigma) that had been preincubated for 10 min at 4 °C in 10 mM Tris, pH 7.0, 600 mM NaCl, and 1 mM EDTA. Reactions were performed in a 96-well plate that was placed on ice under a 302-nm UV-light source (115 V, 60 Hz, and 160 mA) at a distance of approximately 4 cm. Samples were exposed to UV light for 10 min, mixed with 3× load buffer (150 mM Tris, pH 6.8, 30% (v/v) glycerol, 6% (w/v) sodium dodecyl sulfate, 0.3% (w/v) bromophenol blue) and electrophoresed for 70 min at 130 V on a 15% denaturing polyacrylamide gel. Gels were then stained with ethidium bromide to allow detection of the RNA, followed by Coomassie staining to visualize protein.

Duplex formation

5′-fluorescein-labeled RNA was purchased from Dharmacon Research Inc., and analysis of the RNAs by mass spectroscopy indicated that >90% of the RNAs contained fluorescein. RNA strands with no fluorescein were synthesized by in vitro runoff transcription reactions using DNA templates that contained the T7 promoter element 5′-TATAGTGAGTCGTATTA-3′ upstream of the coding sequence. Prior to in vitro transcription reactions, DNA templates were annealed with an equi-molar amount of the complementary T7 primer (5′-TAATACGACTCACTATAG-3′).

The nucleotide sequences of the two strands in the RNA duplexes used in the gelFRET assays are shown in Figure 1. The strands were annealed by slow cooling from an initial temperature of 85 °C to room temperature over a 2-h period. Annealing was performed in the dark (to avoid bleaching of fluorescein) with approximately 45 μM of the two complementary strands in 1 mM EDTA, 10 mM Tris, pH 8.0, and 100 mM KCl. RNA duplexes were stored at −20 °C. Individual aliquots of duplex were only used once to avoid freeze-thaw and degradation. The first three base pairs at the top of the duplex stem differ from those in SLII to maximize the transcriptional yield of each strand while maintaining the same base-pair composition between the stems of the RNA duplex and SLII.

Affinity constants for binding of FinO to either SLII or RNA duplex were obtained by gel electrophoretic mobility shift assays, essentially as described previously (Ghetu et al., 1999).

GelFRET assay

Texas Red C5 bromoacetamide (TR, Molecular Probes) was dissolved in DMSO to a final concentration of 20 mM, divided into 10-μL aliquots, and stored at −20 °C in the dark. For modification of the cysteine point mutants, 100 μL of protein at a concentration of 10 μM in 50 mM Tris, pH 8.0, 600 mM NaCl, and 1 mM EDTA was mixed with 1 μL of 20-mM TR and incubated at room temperature for 2 h. The reaction mixture was subsequently separated over a BioRad P30 spin-column to remove unincorporated TR. Some free TR passed through the spin column with the protein, with the amount getting through varying from sample to sample. This did not affect the gel-FRET results, as free TR had a different electrophoretic mobility than the nucleoprotein complexes (Fig. 4A). FinO-RNA complexes were formed by the incubation of ~500 nM of protein with 370 nM of duplex, in 50 mM potassium phosphate, pH 7, 450 mM NaCl, and 15% sucrose at 4 °C for at least 10 min. The complexes were then separated from free components by native 10% PAGE at 4 °C and 250 V for 3 h. The gels were analyzed using a FluorImagerFSI fluorescence scanner (Molecular Dynamics), with a 488-nm argon ion laser to excite the fluorescein on the RNA, a 530 ± 15-nm band pass filter to detect fluorescein fluorescence, and a 610-nm long-pass filter to detect TR fluorescence. Calibration standards containing only donor or acceptor fluorophores were used to determine the ratio of fluorescence emissions for each fluorophore through each filter.

To determine the percentage of Texas Red modified protein, TR-reacted proteins were first separated from free TR by 15% SDS-PAGE, and visualized by UV excitation of Texas Red or Coomassie staining. The intensity of the protein bands, upon UV excitation, were normalized to the intensity of Coomassie stained bands, assuming that the R165C mutant, which displayed the highest ratio of UV excitation intensity to Coomassie intensity of all the mutants, was 100% modified. We estimate that all mutants were at least 60% modified.

ACKNOWLEDGMENTS

We thank Vladimir Ramirez-Carrozzi for assistance with gel-FRET experiments and Kevin Wilson and Ross Edwards for critical reading of the manuscript. This work was supported by grants from the Canadian Institutes of Health Research and the Alberta Heritage Foundation for Medical Research.

Received November 15, 2001; returned for revision January 3, 2002; revised manuscript received March 29, 2002

REFERENCES

Chen Y, Ebright RH. 1993. Phenyl-azide-mediated photocross-linking analysis of Cro-DNA interaction. *J Mol Biol 230*:453–460.

Diebold RJ, Rajaram N, Leonard DA, Kerppola TK. 1998. Molecular basis of cooperative DNA bending and oriented heterodimer binding in the NFAT1-Fos-Jun-ARRE2 complex. *Proc Natl Acad Sci USA 95*:7915–7920.

Finnegan D, Willetts N. 1972. The nature of the transfer inhibitor of several F-like plasmids. *Mol Gen Genet 119*:57–66.

Frost LS, Ippen-Ihler K, Skurray RA. 1994. Analysis of the sequence and gene products of the transfer region of the F sex factor. *Microbiol Rev 58*:162–210.

Ghetu AF, Gubbins MJ, Frost LS, Glover JN. 2000. Crystal structure of the bacterial conjugation repressor FinO. *Nat Struct Biol 7*: 565–569.

Ghetu AF, Gubbins MJ, Oikawa K, Kay CM, Frost LS, Glover JN. 1999. The FinO repressor of bacterial conjugation contains two RNA binding regions. *Biochemistry 38*:14036–14044.

Hall KB, Fox RO. 1999. Directed cleavage of RNA with protein-tethered EDTA-Fe. *Methods 18*:78–84.

Ho SN, Hunt HD, Horton RM, Pullen JK, Pease LR. 1989. Site-directed mutagenesis by overlap extension using the polymerase chain reaction. *Gene 77*:51–59.

Jerome LJ, Frost LS. 1999. In vitro analysis of the interaction between the FinO protein and FinP antisense RNA of F-like conjugative plasmids. *J Biol Chem 274*:10356–10362.

Jerome LJ, van Biesen T, Frost LS. 1999. Degradation of FinP antisense RNA from F-like plasmids: The RNA-binding protein, FinO, protects FinP from ribonuclease E. *J Mol Biol 285*:1457–1473.

Koraimann G, Koraimann C, Koronakis V, Schlager S, Hogenauer G. 1991. Repression and derepression of conjugation of plasmid R1 by wild-type and mutated finP antisense RNA. *Mol Microbiol 5*:77–87.

Koraimann G, Teferle K, Markolin G, Woger W, Hogenauer G. 1996. The FinOP repressor system of plasmid R1: Analysis of the antisense RNA control of traJ expression and conjugative DNA transfer. *Mol Microbiol 21*:811–821.

Lee SH, Frost LS, Paranchych W. 1992. FinOP repression of the F plasmid involves extension of the half-life of FinP antisense RNA by FinO. *Mol Gen Genet 235*:131–139.

Leonard DA, Kerppola TK. 1998. DNA bending determines Fos-Jun heterodimer orientation. *Nat Struct Biol 5*:877–881.

Mazodier P, Davies J. 1991. Gene transfer between distantly related bacteria. *Annu Rev Genet 25*:147–171.

Mullineaux P, Willetts N. 1985. Promoters in the transfer region of plasmid F. *Basic Life Sci 30*:605–614.

Pendergrast PS, Chen Y, Ebright YW, Ebright RH. 1992. Determination of the orientation of a DNA binding motif in a protein-DNA complex by photocrosslinking. *Proc Natl Acad Sci USA 89*:10287–10291.

Ramirez-Carrozzi V, Kerppola T. 2001a. Gel-based fluorescence resonance energy transfer (gelFRET) analysis of nucleoprotein complex architecture *Methods 25*:31–43.

Ramirez-Carrozzi VR, Kerppola TK. 2001b. Long-range electrostatic interactions influence the orientation of Fos-Jun binding at AP-1 sites. *J Mol Biol 305*:411–427.

Ramirez-Carrozzi VR, Kerppola TK. 2001c. Dynamics of Fos-Jun-NFAT1 complexes *Proc Natl Acad Sci USA 98*:4893–4898.

Ramirez-Carrozzi VR, Kerppola TK. 2001d. Control of the orientation of Fos-Jun binding and the transcriptional cooperativity of Fos-Jun-NFAT1 complexes. *J Biol Chem 276*:21797–21808.

Sandercock JR, Frost LS. 1998. Analysis of the major domains of the F-fertility inhibition protein, FinO. *Mol Gen Genet 259*:622–629.

van Biesen T, Frost LS. 1994. The FinO protein of IncF plasmids binds FinP antisense RNA and its target, *traJ* mRNA, and promotes duplex formation. *Mol Microbiol 14*:427–436.

van Biesen T, Soderbom F, Wagner EG, Frost LS. 1993. Structural and functional analyses of the FinP antisense RNA regulatory system of the F conjugative plasmid. *Mol Microbiol 10*:35–43.